A dielectrophoresis-impedance method for protein detection and analysis

Ahmad Sabry Mohamad, Roszymah Hamzah, Kai F. Hoettges, and Michael Pycraft Hughes

A dielectrophoresis-impedance method for protein detection and analysis

Ahmad Sabry Mohamad,[1,2,a] Roszymah Hamzah,[3] Kai F. Hoettges,[2,b] and Michael Pycraft Hughes[2]

[1]*Medical Section, Universiti Kuala Lumpur-British Malaysian Institute, Bt. 8 Jalan Sungai Pusu, 53100 Gombak, Selangor, Malaysia*
[2]*Centre for Biomedical Engineering, University of Surrey, Guildford GU2 7XH, Surrey United Kingdom*
[3]*Ampang Hospital, Jalan Pandan Mewah, 68000 Ampang, Selangor, Malaysia*

Dielectrophoresis (DEP) has increasingly been used for the assessment of the electrical properties of molecular scale objects including proteins, DNA, nanotubes and nanowires. However, whilst techniques have been developed for the electrical characterisation of frequency-dependent DEP response, biomolecular study is usually limited to observation using fluorescent markers, limiting its applicability as a characterisation tool. In this paper we present a label-free, impedance-based method of characterisation applied to the determination of the electrical properties of colloidal protein molecules, specifically Bovine Serum Albumin (BSA). By monitoring the impedance between electrodes as proteins collect, it is shown to be possible to observe multi-dispersion behaviour. A DEP dispersion exhibited at 400 kHz is attributable to the orientational dispersion of the molecule, whilst a second, higher-frequency dispersion is attributed to a Maxwell-Wagner type dispersion; changes in behaviour with medium conductivity suggest that this is strongly influenced by the electrical double layer surrounding the molecule. *© 2017 Author(s). All article content, except where otherwise noted, is licensed under a Creative Commons Attribution (CC BY) license (http://creativecommons.org/licenses/by/4.0/).* [http://dx.doi.org/10.1063/1.4974290]

I. INTRODUCTION

For more than fifty years, dielectrophoresis (DEP) has been used for the manipulation of a variety of particles, both organic and inorganic, and for myriad applications including separation, fabrication and analysis.[1,2] First described by Herbert Pohl in 1951, DEP is the motion of a particle due to its polarization in the presence of non-uniform electric field.[3] The magnitude and direction of the DEP force is regulated by the relative polarizability of the particle, which depends on the dielectric properties of both the particle and the suspending medium, as well as the frequency of the energising field.

Recently, DEP has gained significant interest for the manipulation of molecules and nanostructures. For many years it was believed that DEP force, which scales according to the volume of the manipulated particle, was too small at molecular levels to overcome Brownian motion; nevertheless, the first demonstration of DEP manipulation of biomolecules was exhibited by Masao Washizu and co-workers in 1994.[4] Since this time, a number of demonstrations of biomolecular DEP have been performed, many of which are reviewed elsewhere.[5] More recent developments include the use of DEP to study conduction mechanisms in DNA;[6] Kim et al. demonstrated positive DEP established to sensing biomolecules.[7] Kotsuki et al. recently published organic semiconductor single crystals formed a field effect transistor using DEP,[8] and lately in 2016, there were also inorganic DEP

---

[a]Correspondence: sabry@unikl.edu.my, Tel.: +06-012-949-7800

[b]Present address: Department of Electrical Engineering and Electronics, University of Liverpool, Liverpool.

7, 015202-1

manipulations of particle such nanotubes and silver nanoparticle demonstrated such as Liang et al. and Leiterer et al.[9–11]

Serum Albumin has been one of the most extensively studied proteins in blood plasma. Some of the albumins most commonly studied are human serum albumin (HSA) rat serum albumin (RSA) and bovine serum albumin (BSA),[12] which are widely available at high purity and low cost. Serum albumin is a soluble multi-domain protein, without prosthetic group subjoin of carbohydrates that is absolutely stable; the primary structure is prolate elliptical in shape, with dimensions 140x40nm[13] with a low intrinsic viscosity. Their molecular weight is about 66200 D, in cysteine group (Cys-34) and low tryptophan content. Albumin helps in transport of drugs and ligands by binding to it and so reduces the free serum concentration of these compounds. Competitive binding of drug may occur at the same site or different sites (conformational changes) for example warfarin as anticoagulant and diazepam as derivative drug. Therefore, serum albumin acts as carriers for numerous exogenous and endogenous compounds.[14] The primary structure of BSA is composed of 528 amino acid residues. The sequences have 17 disulphate bonds resulting in nine formed by the bridges. BSA contains of Asparagine, Glutamine, Alanine, Leucine and Lysine as well as the four amino acid residues in the sequence of Glycine-Phenylalanine-Glycine-Asparagine.[15]

Typically, experiments where DEP has been used to analyse the medium conductivity-dependent behaviour of biological macromolecules have been performed using fluorescent microscopy,[5] whereas characterisation of nanoscale particles such as carbon nanotubes[16] and zinc oxide nanowires[17,18] has employed impedance measuring techniques; impedance methods have been used for the study of larger particles such as cells,[19] but have never previously been applied to biological nanoparticles. In this paper, we present for the first time and impedance-based method for the determination of the electrical properties of dissolved biomolecules, using serum albumin as a model.

II. MATERIALS AND METHODS

A. Protein solution

Solutions of bovine serum albumin (30 mg) were prepared by dissolving into 3 ml sodium carbonate (Na_2CO_3) buffer. 8 mg ammonium chloride (NH_4Cl) was added and the solution incubated for 2 hours at 4°C. The pH of this solution was adjusted to >8.0 by adding NaOH (the iso-electric point of BSA is <5, ensuring no conformational or similar surface charge effects were observed). Media conductivity of every samples recorded varies range from 1.1 mS/m minimum to 281.0 mS/m maximum. Finally, 120 μl glycerol were mixed into protein solution to enhance stability. All of the items were purchased from Sigma-Aldrich UK. A digital conductivity meter unit was used to measure the solution. The protein solution then filtered by Millipore membrane 0.22 μm with 5 ml syringe. Twelve samples were prepared at various conductivities to investigate their behaviours. Experiments were performed in laboratory with room temperature. Each experiment was replicated 3 times.

B. Measurement apparatus

DEP impedance spectroscopy of protein collection conducted using micro-electrodes, configured with an impedance analyser device. Electrodes were of a standard quadrupole geometry and fabricated of 100 nm Au on a 10nm Ti seed layer on glass (as shown in Figure 1); full details of the geometry and fabrication methods are available elsewhere.[6] A resistance was connected in series with the electrodes, and the voltage across the resistor and electrode was measured using a NumetriQ analyser phase multimeter and impedance analyser (N4L, Leicester, UK). The impedance analyser was used a 4-terminal configuration to connect to the polynomial micro-tip electrode. This allowed the NumetriQ phase analyzer multimeter and impedance analyzer to apply current to the electrode with one pair of terminals (High Drive and High Sense) and (Low Drive and Low Sense), as shown in Figure 1. Dielectrophoresis was performed by applying AC electric fields at frequencies between 100 kHz and 16 MHz logarithmic spaced with 5 points per decade, with an applied voltage of 5 Vp-p. To record a single data point the electrodes were energised at a set frequency, then a 5 μl drop of the BSA solution was deposited to the middle of paired micro-electrode. Immediately upon the solution reaching the electrodes, the impedance was observed to exhibit a negative exponential change in impedance. The
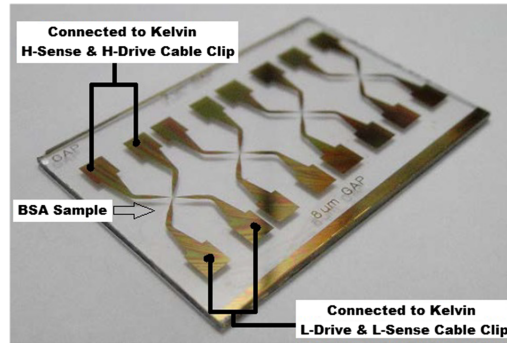
FIG. 1. Impedance measurement was setup in serial circuit diagram.

time constant of the change of resistance was determined after 300 seconds of recording. A typical deposition time of 5 minutes was then followed by rinsing the sample with methanol and gently blowing the drop off the surface. The experiment was repeated on micro-electrode at five frequencies per decade. The electrodes were connected using a Kelvin clip cable with one pair of terminals, HDrive/HSense (High Drive/High Sense), LDrive/LSense (Low Drive/Low Sense) as second pair of terminal connected to the second clip.

C. Data analysis

When particles experience positive DEP, those nearest the electrodes move rapidly to collect at the electrodes, depleting the region in the electrodes' immediate vicinity; over time, particles are collected from further and further away. This leads to a reduction in particle collection over time, which has been previously phenomenologically modelled as an exponential with time constant τ; as the particles accumulate in the inter-electrode gap, they alter (lower) the inter-electrode impedance as a negative exponential, allowing the determination of τ and hence the relative force at that frequency. By mapping the variation of τ as a function of frequency (but with constant particle concentration) it is possible to determine the DEP collection rate of the particles. This technique was originally developed for carbon nanotubes[16] and nanowires,[19] where it was found that conduction around the electrical double layer[20] dominated the DEP response of particles in this size regime.

The impedance change between the micro-electrodes at 1 second intervals was modelled using the following expression:

$$V_T = V_{Max} \left(1 - e^{-\frac{t}{\tau}} \right) \tag{1}$$

$$V_T = V_{Max} \left(e^{-\frac{t}{\tau}} \right) \tag{2}$$

$$R_T = R_{Max} \left(1 - e^{-\frac{t}{\tau}} \right) \tag{3}$$

$$\frac{R_T}{R_{Max}} = \left(e^{-\frac{t}{\tau}} \right) \tag{4}$$

when $e^y = x$ is equal to $y = ln\ x$ gives Equation 4 into Equation 5:

$$\frac{-t}{\tau} = ln \left(\frac{R_T}{R_{Max}} \right) \tag{5}$$

$$-t = ln \left(\frac{R_T}{R_{Max}} \right) \tau \tag{6}$$

and

$$\tau = \frac{-t}{ln \left(\frac{R_T}{R_{Max}} \right)} \tag{7}$$

The time constant τ of the impedance change data was determined using a Matalb curve fitting toolbox, as described elsewhere.[16,19] The inverse of the time constant was then used to approximate the DEP force, as collection rate is inversely proportional to the force causing the particles to collect.

III. RESULTS

Figure 2 shows the inverse time constant for two medium conductivities, 1.1 and 100 mS/m. As can be seen, both plots exhibit two-dispersion characteristics, similar to those seen in collection of carbon nanotubes measured using the same method.[16] In that case, the populations were attributed to conducting and semiconducting fractions. Here, two dispersions could be observed in the BSA spectrum, and in different proportions at different medium conductivities. .

Figure 3 shows the variation of DEP collection as a function of both medium conductivity and frequency. Both dispersions appeared to exhibit conductivity-dependent behaviour, with the "lower frequency" dispersion appearing to exhibit a resonance-type effect around 150mS/m, but reducing in intensity above this, whilst the "higher frequency" dispersion rises to a peak at around the same mark before reducing slowly.

IV. DISCUSSION

Determination of the dielectric properties of dissolved molecules using a DEP model based on Maxwell-Wagner dispersion principles requires a number of assumptions to be made about the behaviour both of the molecule and the motion of charges around it; nevertheless, we can attempt to interpret the spectrum in order to gain some meaningful insight. Our ellipsoidal molecule can be modelled as ellipsoidal solid particle with major axis r_1 and minor axis r_2, wherein the force is given by

$$F_{Rod} = \frac{2\pi r_1 r_2^2 \varepsilon_m}{3} \mathrm{Re} \left[\frac{\varepsilon_p^* - \varepsilon_m^*}{\varepsilon_m^*} \right] \nabla E^2 \qquad (8)$$

Where ε_m is the suspending medium permittivity, E is the electric field, ∇ is the differential vector operator, $\varepsilon*_p$ and $\varepsilon*_m$ are the complex permittivities of the particle and medium respectively (given by $\varepsilon^* = \varepsilon - {j\sigma}/{\omega}$ where σ represents conductivity, ε permittivity, ω angular frequency and *j* the square root of -1, and the subscripts m and p refer to the medium and protein respectively.

There are a number of possible explanations for the two observed dispersions. The two most likely are the presence of two populations, or the presence of two different dispersion mechanisms active in this frequency region. Analysis of the dielectric properties of serum albumin by Bone et al.,[21] has suggested two populations representing the molecule in one of two distinct orientations towards the applied electric field. Alternatively, the dispersion could be due to other, non-Maxwell-Wagner
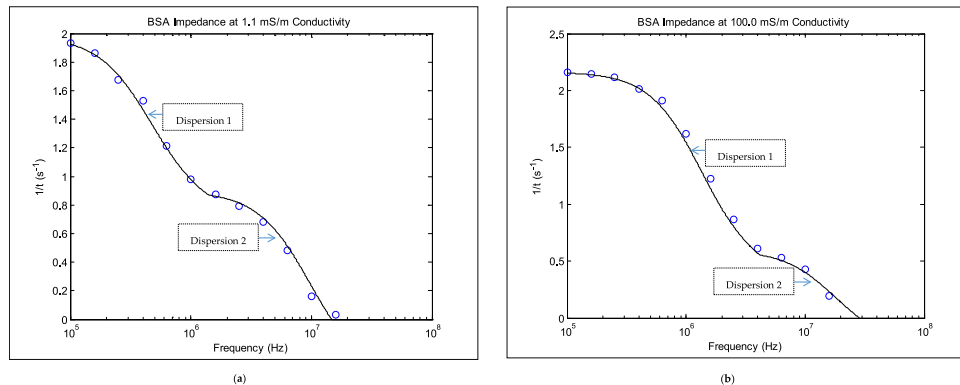

FIG. 2. The plot of $1/\tau$ for BSA impedance at conductivities of (a) 1.1 mS/m and (b) 100 mS/m.
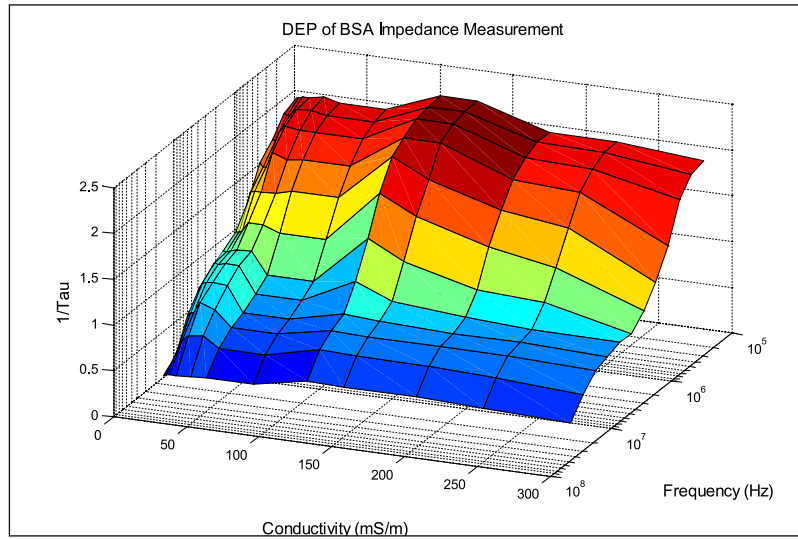
FIG. 3. Variation in $1/\tau$ as a function of both medium conductivity and frequency.

processes. According to Grant and Pethig[22–24] the characterization of relaxation time of dielectric dispersion can be calculated as:

$$\varepsilon_s = \varepsilon' \frac{f_\beta^2(\varepsilon_0 - \varepsilon')}{f^2} \tag{9}$$

Hence ε_0 is dielectric constant, β is relaxation of protein molecules and f is frequency respectively. Grant identified a dielectric dispersion in Bovine Serum Albumin and suggested that orientation dispersion occurs at 400 kHz due to the relaxation of protein molecules.[23]

Examination of figures 2 and 3 suggests that the "lower frequency" dispersion is centred almost exactly on 400 kHz, suggesting that this "population" more likely the orientation dispersion of the protein molecules. The orientation dispersion should not be affected by the conductivity of the medium, but this dispersion does appear to change around 100-150 mS/m; however, since the two dispersions interact, the appearance of a "resonance" effect may in fact be due to the second, "higher frequency" dispersion. This appears to exhibit a rising value of conductivity with increasing medium conductivity, a feature widely noted to be related to increased charge density in the electrical double layer with increasing frequency due to the reduction of the Debye length.[6,16,20]

The overall effect of each of these polarisation process (orientational and interfacial) is to produce a number of dispersions and in the dielectric permittivity of the DEP system. DEP dispersions can be affected by conductivity when a low frequency dispersion seen in the collection of nanoparticles;[20] in particular, there is a "resonant" conductivity where the conductivity of the particles increases at a certain medium conductivity. This kind of resonant frequency was observed at $100 - 150 mS/m$ in the BSA data, indicating that the higher-frequency dispersion can be considered as DEP, and the lower-frequency dispersion is orientation. The DEP dispersion is therefore, caused by the polarisation of the double layer around the molecules, and the "resonance" occurs because the double layer becomes thinner and contains a higher charge density at higher medium conductivities. "Population 1" is instead linked with the orientation of the molecule.

According to de Levine *et al.*,[25] aqueous electrolyte solutions are ionic conductors and are hostile to electrons. Consequently, at the interface between an electrode and an aqueous electrolyte solution, there is mismatch in the type of charge carrier used. In the absence of chemical mechanism to convert one type of charge carrier into the other, the interface behaves as a capacitance.[20] Moreover, AC polarization reduces the threshold electric field potential across the gap which in turn reduces the dielectrophoretic trapping.

Modelling the DEP results from dispersion 2 alone, produce the data shown in Table I. As can be see, the conductivity exhibits a rise of almost x2, peaking around 100mS/m before reducing

TABLE I. Estimated dielectric parameters for BSA derived from modelling.

Sample Conductivity (mS/m)	Population 2 Permittivity ε_0	Population 2 Conductivity (mS/m)
1.1	2.5	0.015
3.2	2.6	0.016
5.6	2.7	0.018
10.0	2.8	0.020
20.0	2.9	0.022
31.0	3.0	0.025
63.0	3.5	0.024
100.0	5.0	0.045
125.0	4.5	0.035
175.0	3.5	0.030
221.0	3.0	0.025
281.0	2.5	0.015

at higher conductivities in line with previously observed behaviour. A rise in particle permittivity was also observed, which is less anticipated, but which may be due to limitations in the model in approximating the shape of the molecule, or in our understanding of the physics of the double-layer behaviour surrounding dissolved molecules in electric fields. Previous studies of molecules using DEP, such as the study of avidin molecules as a function of medium pH,[26] would benefit from this rapid and low-cost method of assessing the dielectric properties of biomolecules.

V. CONCLUSIONS

We have demonstrated that DEP manipulation can be used to determine the dielectric properties of dissolved molecules. The electrical impedance based on the time function could be a rapid label-free approach to determine protein characteristics. As presented in this study, the impedance of the electrode-electrolyte interface and the electrochemical effect (polarization of the electrode) were feasible to distinguish dispersions, which can be attributed to the orientational dispersion of the molecule, plus a Maxwell-Wagner type dispersion governed principally by the countercharge surrounding the molecule. The principle should also be applicable to the measurement of a wide variety of other macromolecules including proteins and DNA.

ACKNOWLEDGMENTS

CONFLICTS OF INTEREST

The authors declare no conflict of interest. The founding sponsors had no role in the design of the study; in the collection, analyses, or interpretation of data; in the writing of the manuscript, and in the decision to publish the results.

[1] M. P. Hughes, "Fifty years of dielectrophoretic cell separation technology," Biomicrofluidics **10**(3), 032801 (2016).
[2] R. Pethig, "(Invited) Where Is Dielectrophoresis (DEP) Going?," Meeting Abstracts. No. 51. The Electrochemical Society, 2016.
[3] H. A. Pohl, "The motion and precipitation of suspensoids in divergent electric fields," Journal of Applied Physics **22**(7), 869–871 (1951).
[4] M. Washizu *et al.*, "Molecular dielectrophoresis of biopolymers," IEEE Trans. Ind. Appl. **30**, 835–843 (1994).
[5] A. Nakano and A. Ros, "Protein dielectrophoresis: Advances, challenges and applications," Electrophoresis **34**, 1085–1096 (2013).
[6] A. Sabry Mohamad *et al.*, "Dielectrophoretic response of DNA shows different conduction mechanisms for poly(dG)-poly(dC) and poly(dA)-poly(dT) in solution," IEEE Transactions on Nanobioscience **13**, 51–54 (2014).

[7] H. Jin Kim *et al.*, "Sensitivity improvement of an electrical sensor achieved by control of biomolecules based on the negative dielectrophoretic force," Biosensors and Bioelectronics **85**, 977–985 (2016).

[8] K. Kotsuki, S. Obata, and K. Saiki, "Self-aligned growth of organic semiconductor single crystals by electric field," Langmuir **32**(2), 644–649 (2016).

[9] Y. Liang, J. Xia, and X. Liang, "Short channel carbon nanotube thin film transistors with high on/off ratio fabricated by two-step fringing field dielectrophoresis," Science Bulletin **61**(10), 794–800 (2016).

[10] C. Leiterer *et al.*, "High precision attachment of silver nanoparticles on AFM tips by dielectrophoresis," Analytical and bioanalytical chemistry **408**(13), 3625–3631 (2016).

[11] C. Leiterer *et al.*, "Dielectrophoresis based integration of nanostructures and their sensorial application," Proc. SPIE (2015).

[12] D. C. Carter and J. X. Ho, "Structure of serum albumin," Advances in protein chemistry **45**, 153–203 (1994).

[13] U. Kragh-Hansen, "Structure and ligand binding properties of human serum albumin," Danish Medical Bulletin **27**, 57–84 (1990).

[14] T. Peters, Jr., *All About Albumin: Biochemistry, Genetics, and Medical Applications* (Academic Press, 1995).

[15] J. R. Brown, "Serum albumin: amino acid sequence," Albumin structure, function and uses, 27–51 (1977).

[16] N. Mureau *et al.*, "In situ and real time determination of metallic and semiconducting single-walled carbon nanotubes in suspension via dielectrophoresis," Applied Physics Letters **88**, 243109 (2006).

[17] C. Opoku *et al.*, "Solution processable multi-channel ZnO nanowire field-effect transistors with organic gate dielectric," Nanotechnology **24**, 405203 (2013).

[18] J. Suehiro *et al.*, "Quantitative estimation of biological cell concentration suspended in aqueous medium by using dielectrophoretic impedance measurement method," Journal of Physics D: Applied Physics **32**(21), 2814 (1999).

[19] M. Constantinou *et al.*, "Simultaneous tunable selection and self-assembly of SI nanowires from heterogeneous feedstock," ACS Nano **10**, 4384–4394 (2016).

[20] M. P. Hughes, "Dielectrophoretic behavior of latex nanospheres: Low-frequency dispersion," Journal of Colloid and Interface Science **250**, 291–294 (2002).

[21] S. Bone *et al.*, "Electronic properties of some protein–methylglyoxal complexes," Proceedings of the National Academy of Sciences **75**(1), 315–318 (1978).

[22] R. Pethig, "Dielectric and electrical properties of biological materials," Journal of Bioelectricity **4**(2), vii–ix (1985).

[23] E. H. Grant, "Dielectric dispersion in bovine serum albumen," Journal of molecular biology **19**(1), 133–139 (1966).

[24] R. Pethig, "Protein-water interactions determined by dielectric methods," Annual review of physical chemistry **43**(1), 177–205 (1992).

[25] S. Levine and G. H. Neale, "The prediction of electrokinetic phenomena within multiparticle systems. I. Electrophoresis and electroosmosis," Journal of Colloid and Interface Science **47**(2), 520–529 (1974).

[26] M. P. Hughes, *Nanoelectromechanics in Engineering and Biology* (CRC Press, Boca Raton, 2002).